

Constraints from luminosity-displacement correlation of high-mass X-ray binaries

Zhao-yu Zuo

School of Science, Xi'an Jiaotong University, Xi'an 710049, China
email: zuozyu@xjtu.edu.cn

Abstract. We have modeled the luminosity-displacement correlation of high-mass X-ray binaries (HMXBs) with an evolutionary population synthesis (EPS) code. Detailed properties including offsets of simulated HMXBs are presented under both common envelope prescriptions usually adopted (i.e., the α_{CE} formalism and the γ algorithm), and several theoretical models describing the natal kicks. We suggest that the distinct observational properties may be used as potential evidence to discriminate between models.

Keywords. stellar evolution, compact stars, X-ray binaries.

1. Introduction

Using data from *Chandra* and NICMOS on board *Hubble* Space Telescope (HST) of X-ray sources and star clusters, respectively, [Kaaret et al. \(2004\)](#) found that: the X-ray sources (number: 66) in three starburst galaxies (M 82, NGC 1569, and NGC 5253) are in general located near the star clusters, and brighter sources are most likely closer to the clusters. Moreover, there is an absence of luminous sources ($L_X > \sim 10^{38} \text{ ergs s}^{-1}$) at relatively large displacements ($> 200 \text{ pc}$) from the clusters (i.e., L_X versus R correlation). In our work, the spatial offsets of HMXBs are modeled for a range of theoretical models describing the natal kicks and the common envelope (CE) evolution.

2. Model

We used the EPS code developed by [Hurley, Pols & Tout \(2000\)](#) and [Hurley, Tout & Pols \(2002\)](#), and updated by [Zuo et al. \(2008\)](#) to calculate the number and X-ray luminosity (L_X) of X-ray binaries (XRBs) and their offsets (R) from the clusters where they were born. We calculated the X-ray luminosity for different kinds of HMXBs as in [Zuo, Li & Gu \(2014\)](#). We adopted the same procedure to compute the binary motion in the cluster potential (i.e., the offset R) as in [Zuo & Li \(2010\)](#).

We constructed seven models to investigate how the spatial offsets of HMXBs are influenced by the natal kicks we adopted. In our basic model (i.e., model BAC), the dispersion of kick velocity σ_{kick} is chosen as 150 km s^{-1} , and we adopted a fallback prescription describing as a modified factor $\eta_{\text{m}} = 1 - f_{\text{b}}$, where f_{b} the fraction of the stellar envelope that falls back, for BH kicks. We also changed σ_{kick} (in units of km s^{-1}) to be 50 (M1), 100 (M2) and 265 (M3) and then fixed the value of σ_{kick} at 150 km s^{-1} and applied three more forms of BH natal kicks (i.e., no natal kicks in model M4, high natal kicks in model M5 and momentum-conserving kicks in model M6, see [Table 1](#)), respectively.

We considered several different choices of the CE parameter α_{CE} (see [Table 2](#)) in order to constrain its value. They are denoted as A02-A10, respectively, where the last two digits correspond to the value of α_{CE} . The maximum value of α_{CE} should be within

Table 1. Summary of natal kick models. Here σ_{kick} is the dispersion of kick velocity, η_m is the modified factor, and f_b is the fraction of the stellar envelope that falls back.

Model	σ_{kick} [km s^{-1}]	η_m	Description for NS	Description for BH
BAC	150	$1 - f_b$	Basic ^a	Fallback; Basic
M1	50	$1 - f_b$	Very low kicks	Fallback; Very low kicks
M2	100	$1 - f_b$	Low kicks	Fallback; Low kicks
M3	265	$1 - f_b$	High kicks	Fallback; High kicks
M4	150	0	Basic	No natal kicks
M5	150	1	Basic	High natal kicks
M6	150	$M_{\text{NS}}/M_{\text{BH}}$	Basic	Momentum-conserving kicks

^a Basic means $\sigma_{\text{kick}} = 150 \text{ km s}^{-1}$.

Table 2. Different models on the treatment of the CE parameter α_{CE} .

Model	A02	A03	A04	A05	A06	A07	A08	A09	A10
α_{CE}	0.2	0.3	0.4	0.5	0.6	0.7	0.8	0.9	1.0

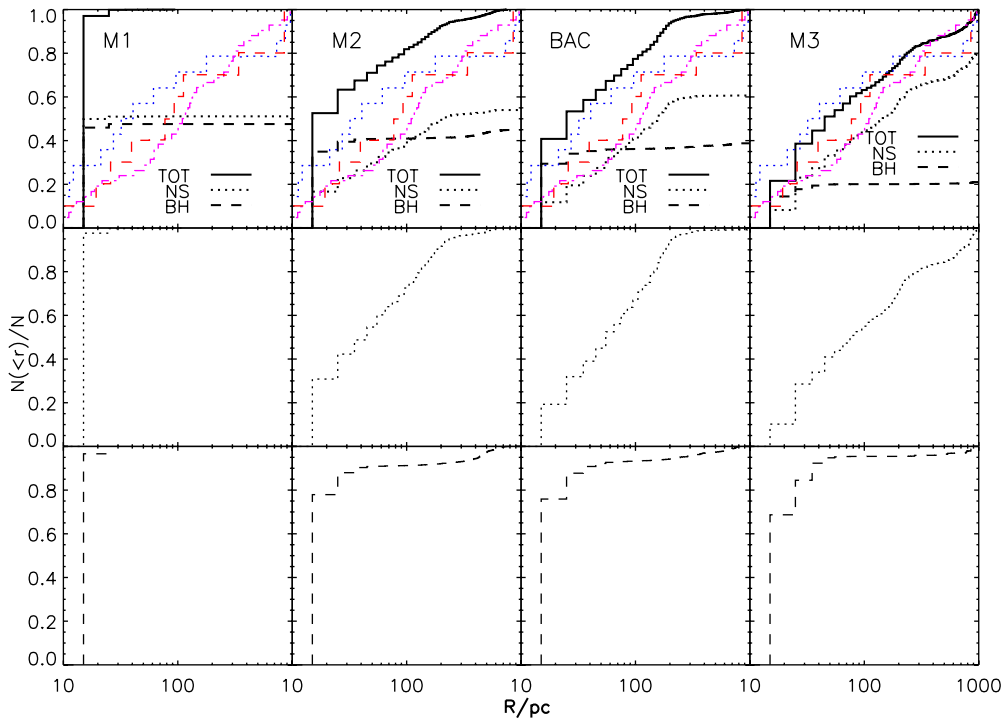


Figure 1. The normalized cumulative distribution for the numbers of ALL-XRBs (top), NS-XRBs (middle), and BH-XRBs (bottom), respectively. From left to right are models M1, M2, BAC, and M3.

unity as the potential internal energies have been considered in the quantity of the binding energy of the envelope (see Xu & Li 2010 and Loveridge *et al.* 2011 for the details).

3. Results

Fig. 1 shows the normalized cumulative distribution of HMXB offsets (top: Total, along with the relative contributions of NS- and BH- HMXBs; middle: NS-HMXBs; bottom: BH-HMXBs) in the luminosity range $10^{36} < L_X < 10^{38} \text{ erg s}^{-1}$ under different choices of σ_{kick} (see Table 1). Only sources with offsets $10 \text{ pc} < R < 1 \text{ kpc}$ are selected according to

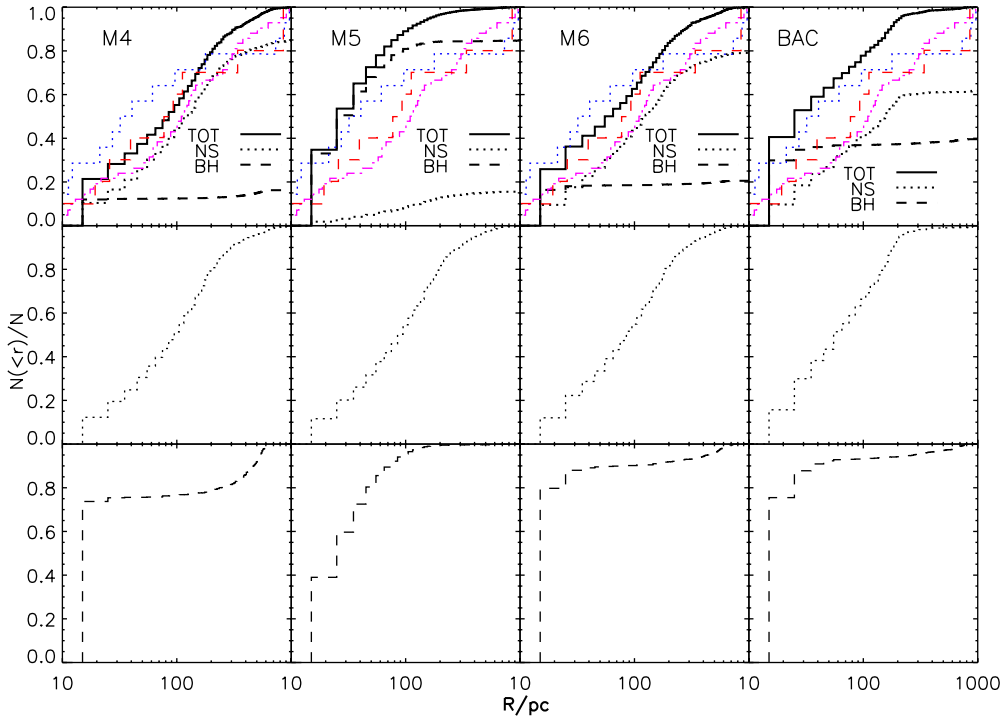


Figure 2. Same as in Fig. 1, but for sources in models M4-M6, and BAC from left to right.

the [Kaaret et al. \(2004\)](#) sample. The thin-solid, dotted, and dashed lines represent the observed cumulative distributions of source displacements in galaxies M82, NGC 1569, and NGC 5253 (see Fig. 2 in [Kaaret et al. 2004](#), similarly hereinafter), respectively. The differences are remarkable. When natal kicks are too weak (i.e., on the order of several tens of km s^{-1} , see model M1), no sufficient sources can be kicked to large displacements from star clusters. In order to be compatible with observations, the value of σ_{kick} should be greater than $\sim 100 \text{ km s}^{-1}$ (see models BAC, M2, and M3).

Fig. 2 is the same as in Fig. 1, but for different treatments on the BH natal kicks (models M4-M6 versus model BAC). It is clear that when full natal kicks are applied to BHs (i.e., model M5), BH HMXBs dominate the whole population in our interested offset region, greatly different from other models and the observational data. These sources are predicted to be mainly long-period BH sources powered by stellar winds from massive ($\sim 30 - 75 M_{\odot}$) MS companions (see Fig. 4 in [Zuo, Li & Gu 2014](#) for a typical evolutionary sequence), which may serve as a potential clue to further discriminate between models of BH natal kicks.

Fig. 3 is the same as in Fig. 1, but under different choices of α_{CE} (see Table 2). Clearly models with α_{CE} between $\sim 0.8 - 1.0$ (i.e., models A08-A10) can match the observation quite closely, while models with $\alpha_{\text{CE}} < \sim 0.4$ clearly fail. In models A02-A04, very few sources can move to 100 pc away from the star clusters, which is in marked contrast with the observations. We note that this result is also consistent with the one obtained through HMXB X-ray luminosity function (XLF) simulations presented by [Zuo & Li \(2014\)](#).

4. Discussion and Conclusions

Our work shows that, using the apparent L_X vs. R distribution of HMXBs, it is possible to investigate the natal kick problem and constrain the value of CE parameter α_{CE} .

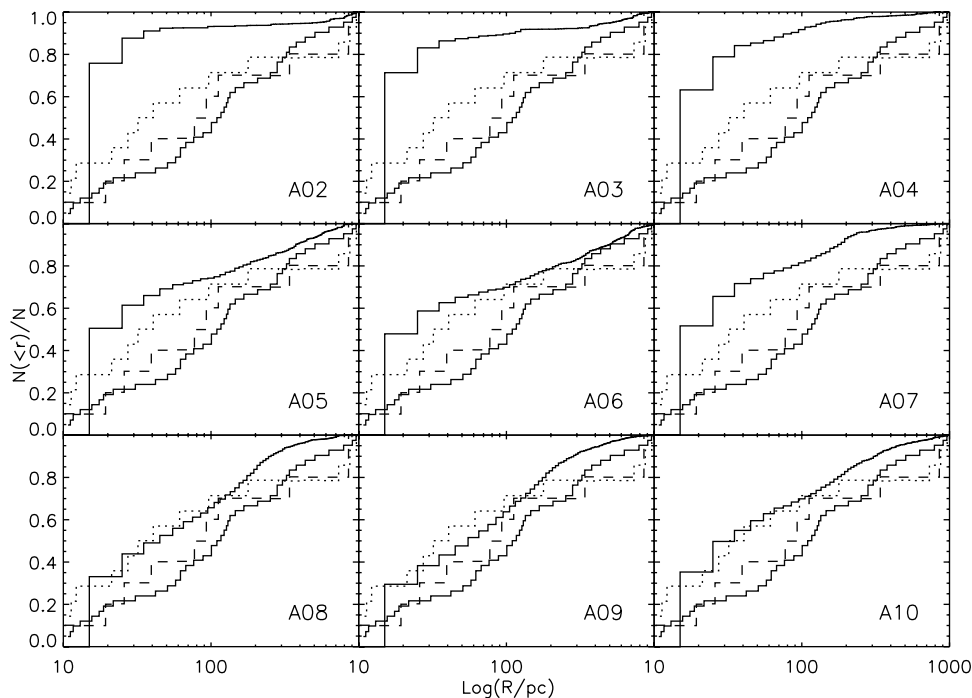


Figure 3. The normalized cumulative distribution (thick-solid line) for models A02–A10, respectively (see Table 2).

The magnitude of σ_{kick} is constrained to be larger than $\sim 100 \text{ km s}^{-1}$, while σ_{kick} on the order of several tens km s^{-1} may be excluded. More importantly, full BH natal kicks (i.e., similar to those that NSs may receive) are likely to be ruled out though it has just been suggested recently by [Repetto, Davies & Sigurdsson \(2012\)](#) to explain the observed distribution of low-mass X-ray binaries with BHs. We also made constraints on the CE efficiency α_{CE} . Within the framework of the standard energy formula for CE and core definition at mass $X = 10$ per cent, a high value of α_{CE} , i.e. around 0.8–1.0, is more preferable, while $\alpha_{\text{CE}} < \sim 0.4$ likely can not reconstruct the observed L_X vs. R distribution.

The results are also subject to some uncertainties and simplified treatments. For example, we did not consider dynamical interactions in our calculation though it may play a non-negligible role in binary formation and kinematics ([Mapelli *et al.* 2013](#)). And when constraining the natal kicks, we only selected one typical value of α_{CE} for simplicity. However CE efficiency is also an important parameter, which may not only affect the system velocity, and hence the spatial offset of the system, but also the whole population of resultant XRBs as well. In addition, the range of α_{CE} we obtained here itself suffers from great uncertainties. It may vary greatly with different assumption describing the CE, such as different core-envelope boundaries, different energy sources used to unbind the envelope, etc.

Acknowledgements

This work was supported by the National Natural Science Foundation of China (grant 11573021), the Natural Science Basic Research Program of Shaanxi Province – Youth Talent Project (No. 2016JQ1016) and the Fundamental Research Funds for the Central Universities.

References

- Hurley, J. R., Pols, O. R., & Tout, C. A. 2000, *MNRAS*, 315, 543
- Hurley, J. R., Tout, C. A., & Pols, O. R. 2002, *MNRAS*, 329, 897
- Kaaret P., Alonso-Herrero A., Gallagher J. S., Fabbiano G., Zezas A. & Rieke M. J. 2004, *MNRAS*, 348, L28
- Loveridge, A. J., van der Sluys, M. V., & Kalogera V. 2011, *ApJ*, 743, 49
- Mapelli, M., Zampieri, L., Ripamonti, E. & Bressan, A. 2013, *MNRAS*, 429, 2298
- Repetto, S., Davies, M. B. & Sigurdsson, S. 2012, *MNRAS*, 425, 2799
- Xu, X. J., & Li X. D. 2010, *ApJ*, 716, 114
- Zuo, Z. Y., Li, X. D., & Liu, X. W. 2008, *MNRAS*, 387, 121
- Zuo, Z. Y., & Li, X. D. 2010, *MNRAS*, 405, 2768
- Zuo, Z. Y., Li, X. D., & Gu, Q. S. 2014, *MNRAS*, 437, 1187 (Erratum: 443, 1889)
- Zuo, Z. Y., & Li, X. D. 2014, *ApJ*, 797, 45